九州大学学術情報リポジトリ
Kyushu University Institutional Repository

Characterization of the Porous Medias' Fluid Flow for Self-powered Micropump

Nur Shamimi Amirah Md Sunhazim
Faculty of Mechanical Engineering, Universiti Teknologi Malaysia

Ummi Aqila Norhaidi
Faculty of Mechanical Engineering, Universiti Teknologi Malaysia

Kamaruzaman, Natrah
Faculty of Mechanical Engineering, Universiti Teknologi Malaysia

Abidin, Ummikalsom
Faculty of Mechanical Engineering, Universiti Teknologi Malaysia

https://doi.org/10.5109/7172302

出版情報：Evergreen. 11 (1), pp.394-401, 2024-03. 九州大学グリーンテクノロジー研究教育センター
バージョン：
権利関係：Creative Commons Attribution 4.0 International

KYUSHU UNIVERSITY

Characterization of the Porous Medias' Fluid Flow for Self-powered Micropump

Nur Shamimi Amirah Md Sunhazim[1], Ummi Aqila Norhaidi[1], Natrah Kamaruzaman[1], Ummikalsom Abidin[1,*]

[1]Faculty of Mechanical Engineering, Universiti Teknologi Malaysia

*Author to whom correspondence should be addressed:
E-mail: ummi@utm.my

(Received May 17, 2022; Revised March 10, 2024; Accepted March 18, 2024).

Abstract: Porous media from filter paper utilizing capillary action is integrated in a self-powered micropump. Characteristic of fluid flow through porous media is a crucial parameter in the development of self-powered micropump with fabrication techniques of xurography and thermal lamination. In this work, the characterization of filter paper grades W40 and W41 was carried out using a scanning electron microscope (SEM) and ImageJ software. The analyses yielded porosity of 70.82% for filter paper W41 and 70.24% for filter paper W40. In the experiments conducted, filter paper W41 resulted greater flow rate than W40 for both free and confined environments. The results are due to the greater pore size of filter paper grade W41 compared to W40. Analysis of pressure differential for filter paper grade W40 is 9.32 Pa in the free environment and 3.84 Pa when confined. Conversely, filter paper W41 exhibits lower pressure disparity of 1.92 Pa and 1.12 Pa in free and confined conditions, respectively. This research provides valuable insights into pressure generation within porous media from capillary action, thus offering potential benefits for the design of self-powered micropumps.

Keywords: self-powered micropump; capillary action; porous media; xurography; thermal lamination

1. Introduction

Microfluidic plays a vital application in biomedical field as small sample and reagent volume requirement, faster processing and economical. This technology consists of mini-size components that improves performances and capacity, which can provide a precise parameter monitoring and accurate analysis[1)2)]. These advantages would be beneficial in developing Lab-on-Chip (LoC) devices by accommodating polymerase chain reaction (PCR) processes into a single microfluidic chip to help in early detection of pandemic and chronic viruses and reducing its costs[3)4)]. To activate a microfluidics device, a micropump is integrated. There are two categories of micropumps used, which are mechanical and non-mechanical.

The main difference of these two micropumps is in its operation's procedure. Mechanical micropump works by utilizing a reciprocating diaphragm that is actuated by a physical actuator to pump the liquid, such as piezoelectric, electrostatic and electromagnetic[5)]. On the other hand, non-mechanical micropump does not consists any moving or vibrating parts in transporting the fluid inside the channel. Even though these types of micropumps help in transporting the fluid, but there are still some drawbacks such as high fabrication cost from soft-lithography technique and requires external power supply.

New methods have been discovered and proposed by some researchers to eliminate the use of the external power to transport the liquid in the microchannels in promoting more sustainable environment[6)]. This new method benefits for those living in remote area, who is having limited electricity supply[7)]. Among the techniques are; hand-operated where the pressure is produced from the outside of the device and self-operated, where the pressure is operated from the inside of the device[8)]. Hand-operated micropump use either syringe or finger actuation[9)10)]. However, fluid flow using hand-operated micropumps are difficult to handle as the forces exerted by the end-users are different.

The self-operated micropump operates with the help of capillary force occurs in the channel[11)]. Possibility of bubble trapping and variation of volume control are its drawbacks. The propose method in replacing capillary micropump is by the effect of pressure generation from porous media pores or filter paper[8)]. Filter paper has been used as efficient filter medium in various fields' applications. Filter paper has multiple holes through and made of interwoven and cross-linked fiber. Primary use of filter paper is in filtering larger particles as in separation

of liquid and solid substances mixture[12]. Whatman filter paper is well known to be used compared to other filter paper as it is more efficient, reliable and high-performance properties[13].

Due to the complex microstructures of porous media, transport processes and parameters are quite challenging [14][15]. However, as the high demand of porous media over the years, many studied have been conducted in order to investigate flow rate control and intrinsic properties of the porous media[16]. Porous materials, permeability, and porosity are the essential factors in characterizing fluid behavior in porous media [17][18]. Permeability, as defined by Graczyk and Matyka, is the ability of a porous media to transport fluid [19]. Many theoretical and experimental work have been done on the fluid flow in porous material to identify the relationship between permeability and other macroscopic features, and it is determined that permeability is related to the porosity and specific surface area as given in Equation 1[20][21].

$$k = \frac{p^3}{cS^2} \qquad (1)$$

Porosity is another important parameter of porous medium as it measures the vacant spaces and it is depending on the structure and texture, which can be calculated using Equation 2. Park et al. had studied the behavior of the fluid flow on the porous medium in pressed paper[22]. With the effect of paper is being pressed, the thickness, porosity and permeability are decreased. This eventually led to the decreasing of fluid flow rate through the paper. Fluid flows on porous medium is described as wicking, which is the process of moving liquid through objects via capillary action. There are two theories that are known for wicking in porous medium that are Darcy's Law and Lucas-Washburn equation.

$$p = 1 - \frac{v'}{v} \qquad (2)$$

Darcy's Law is an equation that describes the fluid flow through a porous medium, discovered by Henry Darcy[19]. Equation 3 depicts the Darcy's Law relationship, which states that flow rate is directly proportional to permeability and pressure drop and indirectly related to the distance between the porous media and the fluid's dynamic viscosity. On the other hand, Lucas-Washburn equation the Lucas-Washburn equation describes the relationship between the position of the visible-wetted front and the square root of time [17]. Fluid contains surface tension, contact angle and dynamic viscosity while porous medium is considered to have capillary tubes with an identical radius, where all of these values can be obtained by applying Equation 4[23].

$$Q = -\frac{kA}{\mu L}\Delta P \qquad (3)$$

$$L^2 = \frac{\gamma \cos(\theta) r}{2\mu} t \qquad (4)$$

In recent study, self-powered imbibing microfluidic pump by liquid encapsulation (SIMPLE) was used to provide specific microchannel flow. SIMPLE micropump is operated with filter paper as the porous media. The effect of liquid wicking and degassing from the porous media activate the fluid flow inside of the microchannel. Flow rate obtained of range between 0.07 to 0.17 μL/s is applicable as part of Point-of-Care (POC) diagnostic chips[24]. Another study was conducted using new concept of SIMPLE, called iSIMPLE device and managed to produced fluid flow rate ranging between 0.0167 to 0.5 μL/s. The study proved that the iSIMPLE device has a potential to be implemented for POC applications[25]. In microfluidic technology, replica molding or soft-lithography have been known to be the standard fabrication technique[26]. However, as the technique is time-consuming and laborious, alternative fabrication technique is developed by using craft cutter or xurography method, which is more user-friendly and reduce the fabrication time[27]. Craft cutter cut the desired shape of a microfluidic channel on a pressure-adhesive (PSA) tape and bonded it between transparency films[24][25][28]. This technique is called xurography and it is proven to be an effective way to create complex geometries[29].

Empirical evidence and understanding on the fluid flow through the porous media and its effect on micropump flow using xurography technique is still insufficient. In this study, the characterization of fluids flow in two different Whatman filter paper under confined and free environment are to be conducted. The fluid wicking behavior, flow rate, permeability, porosity and pressure difference will be analyzed in order to design a controllable microchannel flow from a self-actuated micropump.

2. Methodology

2.1 ImageJ Processing

Image processing software of ImageJ has been used to determine the properties of the filter papers used in this study. Microscopic images of Whatman filter paper grades W40 and W41 was acquired through a scanning electron microscope (SEM). In the preparation of samples, the filter papers were circularly cut with a radius of 1 cm. The SEM captures were digitized and subjected to analysis using ImageJ. Through the ImageJ software, the filter papers' porosity was determined following the procedural steps illustrated in Fig. 1.

2.2 Materials

Two different filter papers were used in this study and the properties of each filter paper are as shown in Table 1.

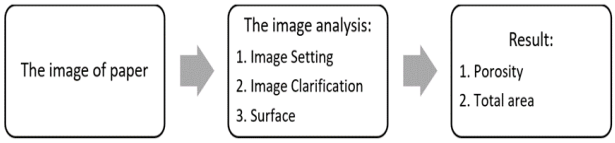

Fig. 1: The image processing process[30].

As the fluid to be absorbed by the filter paper, distilled water was mixed with food colouring was used in other to have good vision of the absorption through the filter paper. In this work, PSA tape was replaced with PVC rigid sheet (0.22 mm thickness) as it functions well from Idris et. al's work. Adoro laminating film (0.15 mm thickness) pouch was used as layers for the sandwich confined environment. The sandwich layers were then thermally laminated.

Table 1. Properties for each filter paper used in the research

Filter Paper	Description	Properties		
		Particle Retention (µm)	Typical Thickness (µm)	Basis Weight (g/m^2)
Grade W40	Medium Flow	8	210	96
Grade W41	Fast Flow	20-25	220	85

2.3 Fabrication Method

The fabrication process began with diamond-shape drawing using Autodesk Auto CAD 2021 software. The design used was from the work of Dosso et al. and as shown in Fig. 2. The diamond-shaped design of filter paper can give a consistent flow at the first expanding part while ensuring a seamless transition at the second restriction part[25]. The diamond shaped design was then converted to DXF file format and transferred to Silhoutte Studio software for the cutting process using Silhoutte Cameo 3-4T cutting machine (USA). This cutting technique is known as xurography.

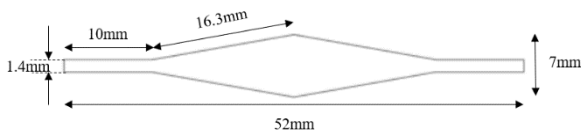

Fig. 2: Design of filter paper with exact dimensions (in mm)

The parameters required for xurography technique are the cutting force and the cutting speed. The finalized parameters for the cutting force, cutting speed and number of passes for PVC rigid sheet were 30, 3 cm/s and 2 respectively. The filter paper was cut manually with scissors after the desired shape was drawn on it.

For the confined environment, the fabrication method was done by combining xurography with thermal lamination. Three layers of sheets were sandwiched with laminate machine (Astar LM-230i, Malaysia) under temperature of 130 degree Celsius as shown in Fig. 3, which the top and bottom layer are the laminating films and the middle layer is the filter paper. The top layer of the laminating films was designed with inlet and outlet holes in order for the distilled water to be absorbed by the filter paper.

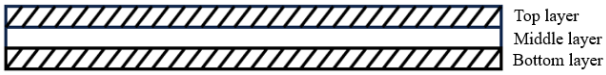

Fig. 3: Cross-sectional of the layer structure for thermal laminating

2.4 Experimental Setup

Sixteen samples for each filter paper used for both environments were fabricated. Figure 4 shows the setup of the wicking experiment, which consists the stopwatch, iPhone X to record and snapshot the whole process, beaker with distilled water mixed with blue dyed food colour and pipette. Since the volume of dyed food colour used is small in order to make the liquid visible, there is no major changes in the water properties. The experimental setup performed was almost the same as the technical manual developed by American Association of Textile Chemists and Colorists[31]. Some changes have been made as the material used in this study is filter paper, instead of fabric.

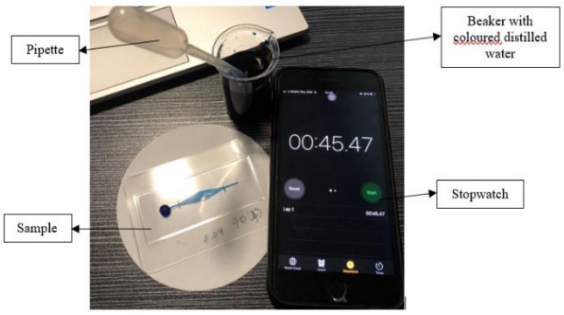

Fig. 4: The experimental setup

Figure 5 shows the whole process of the experiment. There are two sections marked on the filter paper to indicate the start point and end point as shown in Fig. 5(a). A drop of distilled water was dropped at the inlet hole using pipette. The time taken was recorded when the distilled water starts to reach the starting point (Fig. 5(b)) and stopped when it reached the end point (Fig. 5(d)).

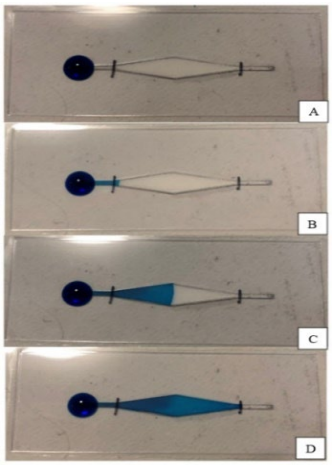

Fig. 5: The operation of the experiment. (A) a droplet at inlet. (B) absorption of water and measurement started. (C) wicking process. (D) experiment was terminated at end point.

3. Results and discussion

3.1 Scanning Electron Microscope (SEM) and ImageJ analysis

The structure of filter paper has multiple holes through and made of interwoven and cross-linked fiber. It is mainly used to filter larger solid particles from liquid particles[32]. By using ImageJ analysis, the structure of the interwoven fiber can be magnified and studied. Image analysis using ImageJ software has been conducted in order to identify porous media properties[33]. Figure 6 and Figure 7 show the SEM images of the filter papers before and after threshold process using ImageJ. Since the size of the filter paper stayed constant, Dosso et al. assumed that the porosity of the filter paper was 70%. The findings of the ImageJ analysis for the filter papers are summarized in Table 2. At 70.82%, filter paper grade W41 has slightly higher porosity percentage than grade W40. Cui et al. observed that density and porosity have an inverse relationship, meaning that a material with fewer pores has a better absorption rate[34]. Thus, it can be concluded that the absorption rate of the filter paper W41 is greater than the W40.

Fig. 6: SEM images for filter paper grade 40 comparison (a) before threshold (b) after threshold

Fig. 7: SEM images for filter paper grade 41 comparison (a) before threshold (b) after threshold

Table 2. Summarization of Particle Analysis

Grade	Pore Average Size (µm)	Porosity (%)
W40	697.13	70.24
W41	413.61	70.82

3.2 Absorption rate of the filter paper

The comparison of the time taken for filter paper grade W40 and W41 for both environment is shown in Fig. 8. For the comparison on the filter papers' grade, filter paper grade W41 requires lesser time compared to filter paper grade W40 for both environments' condition. The percentage difference for both filter paper in free and confined environments are 48% and 79% respectively. This is a result of the filter paper's properties, as filter paper grade W41 has bigger particles than filter paper grade W40. This causes the filter paper grade W41 has more void spaces between the interwoven fibers, that makes the fluid can be easily flow between the voids. Aside from that, filter paper with smaller particle retention size will have trouble absorbing liquid since it comprises a smaller volume of voids or pores. This explains the longer time taken required by filter paper grade W40 to be fully absorbed with distilled water. Another explanation is on the description of the filter papers. Filter paper grade W41 is described as fast flow while filter paper grade W40 is described as medium flow.

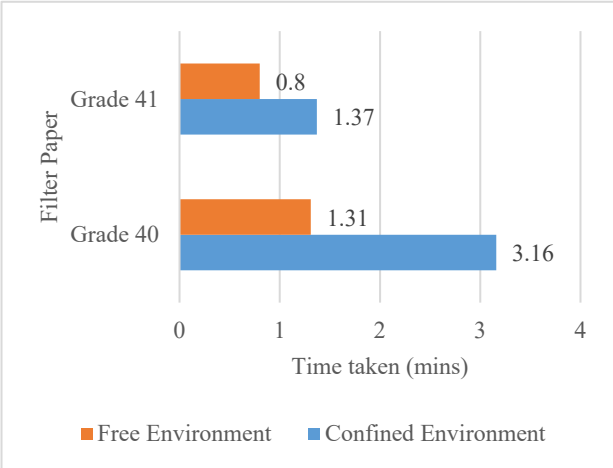

Fig. 8: Time taken comparison of free and confined environments

Another comparison is studied on the environments' condition, where the free and confined environment are compared. The difference between both environment is that the filter paper is laminated between laminating films for confined environment. The percentage difference for free and confined environment for both filter paper is 52% and 83%. The reason of the less flow rate in confined environment is because the filter paper has been pressed down during the lamination process with high pressure and temperature. According to Park et al., once the paper is being pressed down, the thickness, porosity and

permeability of the paper will reduce and causes the fluid flow rate to decrease[21]. The pressed filter paper also has reduced its pore size and thickness. All this effect contributed to slower fluid flow throughout the wet-out process as porous network collapsed and provide high flow resistance.

3.3 Theoretical analysis

Figure 9 shows the comparison of flow rates for each filter papers. Filter paper grade W41 has higher flow rates for both environments compared to grade W40. The flow rate for filter paper grade W41 in free and confined environment is 4.47 µL/min and 2.61 µL/min respectively. In contrast, filter paper grade W40 has flow rates of 2.74 µL/min in free environment and 1.13 µL/min in confined environment. The results obtained was validated and compared to research done by Dosso et al., with the same filter paper used which is Whatman filter paper grade W40[25]. From Dosso et al. study, the average flow rate obtained was 1.20 µL/min while from this study was 1.13 µL/min for the same confined environment. Percentage difference between these results was 5.83 %. Possible caused for the difference is due to different bonding technique used. Dosso et al. study utilized PSA material with adhesive. This is expected as more resistance was imposed by the adhesive on both of filter paper faces and reduce the liquid wicking. On the other hand, this work used thermal lamination techniques for the sandwich polymers configuration and reduce the filter paper faces constraint and be able to provide less flow resistance.

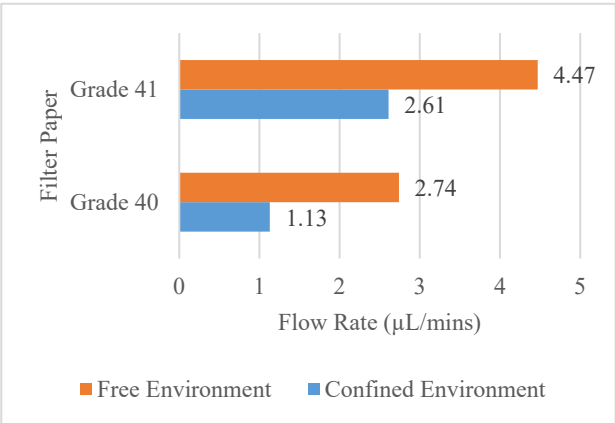

Fig. 9: Flow rate comparison of free and confined environments

The thickness of the filter paper is another factor contributing to the variations in flow rate values. Compared to filter paper grade W40, filter paper grade W41 has a higher flow rate. This is because the flow rate throughout the filter paper can be influenced by the filter paper's length, permeability and thickness[22]. As a result, filter paper grade W41 has higher flow rate as the thickness of the filter paper is 220 µm while grade W40 has a thickness of 210 µm.

Another factor affecting the flow rate in this study is the environment, which are the confined and free environment. As shown in the figure, the flow rate of distilled water is greater in a free environment than in a confined environment. This is due to numerous reasons including the resistance encountered during the absorption process and the filter paper's porosity. For the confined environment, the filter paper is pressed and bonded between lamination film. The lamination film is coated with adhesive that melted once thermal heat is applied and causes the surface became rough and sticky. Thus, liquid that came into contact with the surface of the lamination film had a resistance that slowed down the liquid flow.

Permeability is another important parameter to study the flow of fluid in porous medium, where it measures the ability and capacity of fluid to move around the porous medium[19]. Permeability can be calculated by using Equation 5. Table 3 below are the calculated filter papers' permeability used in this study. High permeability value indicates the porous medium has an easy flow while porous medium with low permeability resists flow. From the calculated permeability obtained, filter paper grade W41 has higher permeability value compared to grade W40 with difference of 0.967 x 10^{-11} m^2. This can be concluded that filter paper grade W41 is able to absorb liquid faster and easier than grade W40.

$$k = \frac{p}{8} R_c^2 \qquad (5)$$

Table 2. Permeability of the filter papers

Filter Paper Grade	Permeability
W40	$k =$ 1.40 x 10^{-12} m^2
W41	$k =$ 1.11 x 10^{-11} m^2

Capillary pressure refers to the pressure difference of two immiscible fluids in a narrow tube. In this study, pressure is generated at the porous media-liquid channel interface. The pressure balance considered in both non-wetting and wetting phase. The pressure of non-wetting phase in this study is defined as the pressure difference across the filter paper (Darcy's Law) whereas the pressure of wetting phase is defined as the pressure difference along the channel (Hagen-Poiseuille). Table 4 shows the capillary pressure calculated for each filter paper using Young-Laplace Equation 6.

$$P_{cap} = \frac{2\gamma \cos(\theta)}{R_c} \qquad (6)$$

Table 4. Capillary pressure of the filter papers

Filter Paper Grade	Capillary Pressure
W40	36.150 kPa
W41	12.853 kPa

The pressure difference for the filter papers were calculated and presented as in Fig. 10 by using Equation 3. According to the Fig. 10, the pressure differentials for filter paper grade W41 in free and confined environments are 1.92 Pa and 1.12 Pa, respectively, whereas for filter paper grade W40, they are 9.32 Pa and 3.84 Pa correspondingly. The pressure difference of the filter paper is directly related to the flow rate of the fluid and inversely proportional to its permeability. Thus, the pressure difference for filter paper grade W41 is higher than grade W40. The percentage difference of the pressure for both filter paper in free and confined environment are 132% and 109%.

In addition, the relationship between capillary pressure and pressure difference of the filter paper can be formulated as in Equation 7. The equation shows that the capillary pressure is inversely proportional to the permeability. As previously said, filter paper with poor permeability restricts and resists fluid flow through it, causing the pressure difference of the filter paper to increase, which finally leads to an increase in capillary pressure.

$$P_{cap} = -\frac{Q\mu L}{kA} + P_w \qquad (7)$$

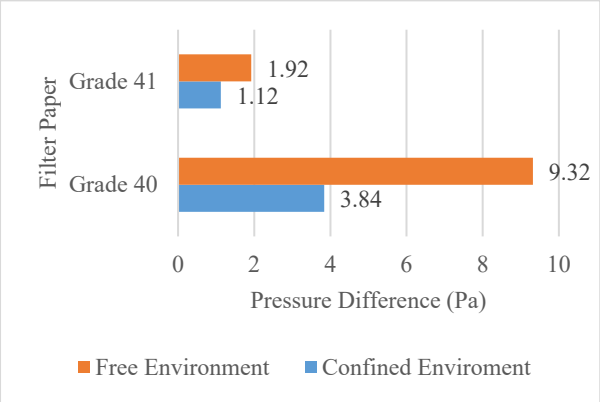

Fig. 10: Pressure difference comparison of free and confined environments of the filter papers

3.4 Horizontal and Vertical Positions of Filter Paper

Wicking experiment was usually done vertically to study the capillary rise on the porous medium, as it will be compared with the Lucas-Washburn model to validate the results. However, most microfluidics devices are used in horizontal position. Thus, a simple experiment was conducted to investigate the impact of the position on the absorption rate of the filter paper. Filter paper was cut to the dimensions of 7 mm × 25 mm. The experiment was done by dropping the liquid onto the filter paper from a fixed height[35]. In the horizontal position, the liquid was dropped on the right side of the filter paper, while in the vertical position, it was dumped on the top, as illustrated in Fig. 11. Figure 12 compares the absorption rates of the filter papers in two different locations, horizontal and vertical.

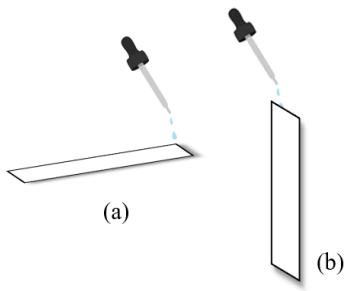

Fig 11: Position of the filter paper and dropper at (a) horizontal position and (b) vertical position

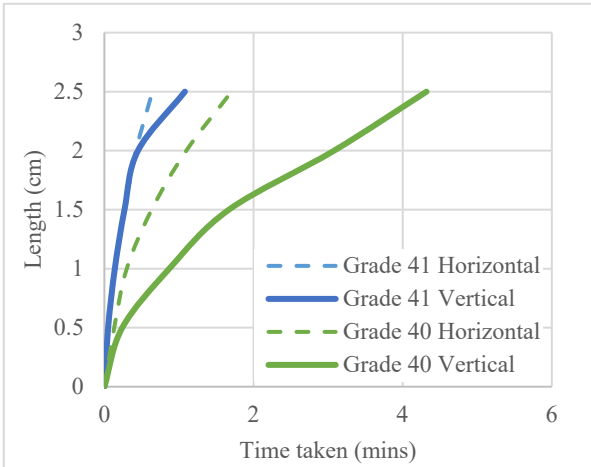

Fig. 12: Absorption rate comparison with positions

The bold line indicates the filter paper in vertical position while dotted line indicates the filter paper in horizontal position. The trend of the graph for each filter paper obtained are similar. From the figure, filter paper grade W40 and W41 requires less time to be fully soaked with distilled water when it is in horizontal position compared to vertical position, which are 0.64 minutes and 1.71 minutes respectively. In vertical position, the time taken for filter paper grade W40 is 4.32 minutes while grade W41 is 1.08 minutes. The percentage difference between filter paper grade W40 and W41 in both positions are 87% and 51% respectively.

In horizontal position, the capillary pressure is greater than the gravitational force, which later will eventually be ignored. In vertical position, due to the gravity that has an opposing effect on the liquid, it causes the fluid flow to slow and stop[36]. A vertical wicking experiment happens when the capillary forces prompt the porous media or the filter paper to absorb the fluid until the balance of gravitational force and equilibrium of the capillary forces is reached[37].

4. Conclusion

In conclusion, the characterization of the fluid flow rate through two different filter papers are successfully studied. Filter paper in confined environment took longer time to be fully absorbed by the distilled water compared to free

environment. This is happened due to pressure and temperature effect during lamination process which alters its' porosity and thickness. Furthermore, the adhesive on the laminating film that is melted during the laminating process provides resistance to fluid flow, particularly on the top and bottom faces of the filter paper. In this study, porosity of filter paper grade W41 is 70.82 % while grade W40 is 70.24 %. Due to its' porosity value and thickness, filter paper grade W41 has improved fluid flow than grade W40. On the other hand, filter paper grade W40 has a greater pressure difference than grade W41. The pressure differential for filter paper grade W40 is 9.32 Pa in free environments and 3.84 Pa when confined, whereas filter paper grade W41 exhibits lower pressure differences of 1.92 Pa and 1.12 Pa in free and confined environments, respectively. Effect of different experiment positions of the filter paper was studied and proved that the horizontal positions give better flow rate as the gravitational force is small or sometimes neglected. This study provides an inside on how fabrication process will influence the fluid flow through the porous media. This study is hope to help in better understanding on how to design a self-actuated micropump for a controllable microchannel flow.

Acknowledgements

The authors would like to thank the Ministry of Education Malaysia for financing this research under the Fundamental Research Grant Scheme, FRGS/1/2019/TK03/UTM/02/2, as well as Universiti Teknologi Malaysia.

Nomenclature

PoC	Point-of-care (–)
PSA	Pressure-sensitive adhesive (–)
SEM	Scanning electron microscope (-)
k	permeability (m^2)
p	porosity (-)
Q	fluid flow rate (m^3/s)
L	penetration length (m)
t	time (s)
A	area (m^2)
P_{cap}	capillary pressure (Pa)
P_{nw}	non-wetting pressure (Pa)
P_w	wetting pressure (Pa)
R_c	pore radius (μm)

Greek symbols

γ	surface tension (N/m)
θ	contact angle (°)
μ	dynamic viscosity (Pa.s)

References

1) "Benefits of Using a Microfluidic Device." n.d. https://www.news-medical.net/life-sciences/Benefits-of-a-Microfluidic-System.aspx (accessed September 28, 2021).
2) I. Ridho, F. Juana, Y. Whulanza, and J. Charmet, "Heating Characterization of Low Energy Consumption Lab-on-a-Chip." *EVERGREEN Journal of Novel Carbon Resources Sciences & Green Asia Strategy,* 8 (*4*), 872-78 (2021). doi.org/10.5109/4742135
3) A.M. Rosli, J.A. Shahir, and R.M. Nizar, "Recent Study on Hard to Machine Material – Micromilling Process." *EVERGREEN Journal of Novel Carbon Resources Sciences & Green Asia Strategy,* 8 (*2*), 445-53 (2021). doi.org/10.5109/4480727
4) N.Z. Zaini, N.B. Kamaruzaman, and U. Abidin, "Magnetic Microbeads Trapping using Microfluidic and Permanent Magnet System," *EVERGREEN Journal of Novel Carbon Resources Sciences & Green Asia Strategy,* 8 (*1*) 156-162 (2021). doi.org/10.5109/4372272
5) S. Mohith, P.N. Karanth, & S.M. Kulkarni, "Recent trends in mechanical micropumps and their applications: A review," *Mechatronics*, 60 34-55 (2019) doi:10.1016/j.mechatronics.2019.04.009
6) M.K. Barai and B.B. Saha, "Energy Security and Sustainability in Japan," *EVERGREEN Journal of Novel Carbon Resources Sciences & Green Asia Strategy,* 2 (*1*) 49-56 (2015). doi.org/ 10.5109/1500427.
7) T. Sato, "How is a Sustainable Society Established?: A Case Study of Cities in Japan and Germany How is a Sustainable Society Established? A Case Study of Cities in Japan and Germany," *EVERGREEN Joint Journal of Novel Carbon Resource Sciences & Green Asia Strategy,* 3 (*2*) 25-35 (2016) doi:10.5109/1800869.
8) J. Park, D.H. Han, and J.K. Park, "Towards practical sample preparation in point-of-care testing: user-friendly microfluidic devices," *Lab on a Chip*, 20 (*7*) 1191-1203 (2020). doi.org/10.1039/D0LC00047G
9) X. Zhang, K. Xia, and A. Ji, "A portable plug-and-play syringe pump using passive valves for microfluidic applications," *Sensors and Actuators B: Chemical,* 304 127331 (2020). doi.org/10.1016/j.snb.2019.127331
10) Y. Whulanza, T.A. Hakim, M.S. Utomo, R. Irwansyah, J. Charmet, and Warjito, "Design and characterization of Finger-Controlled Micropump for Lab-on-a-Chip Devices," *EVERGREEN Journal of Novel Carbon Resources Sciences & Green Asia Strategy,* 6 (*2*) 108-113 (2020). doi.org/10.5109/2321002
11) L. Xu, A. Wang, X. Li, and K.W. Oh, "Passive micropumping in microfluidics for point-of-care testing," *Biomicrofluidics*, 14 (*3*) 031503 (2020). doi.org/10.1063/5.0002169

12) J. Gullichsen, H. Paulapuro, B, Attwood, S. Anne, and G. Smook, n.d. Papermaking Science and Technology Paper and Board Grades Series.
13) H. Kim, M. Prezzi, and R. Salgado, "Calibration of Whatman Grade 42 filter paper for soil suction measurement," *Canadian Journal of Soil Science*, 97 (*2*) 93–98 (2017). doi.org/10.1139/cjss-2016-0064
14) L. Guarracino, T. Rötting, and J. Carrera, "A fractal model to describe the evolution of multiphase flow properties during mineral dissolution," *Advances in Water Resources*, 67 78–86 (2014). doi.org/ 10.1016/j.advwatres.2014.02.011
15) R. Liu, B. Li, and Y. Jiang, "A fractal model based on a new governing equation of fluid flow in fractures for characterizing hydraulic properties of rock fracture networks," *Computers and Geotechnics*, 75 57– 68 (2016). doi.org/ 10.1016/j.compgeo.2016.01.025
16) J.H. Shin, J. Park, S.H. Kim, and J.K Park, "Programmed sample delivery on a pressurized paper," *Biomicrofluidics*, 8 (*5*) (2014). doi.org/ 10.1063/1.4899773
17) E.W. Washburn, "The dynamics of capillary flow," *Physical Review,* 17 (*3*) 273–283 (1921). doi.org/10.1103/PhysRev.17.273
18) E. Fu, S.A. Ramsey, P. Kauffman, B. Lutz, and P. Yager, "Transport in two dimensional paper networks," *Microfluidics and Nanofluidics*, 10 (*1*) 29–35 (2011). doi.org/ 10.1007/s10404-010-0643-y
19) K.M. Graczyk, and M. Matyka, "Predicting porosity, permeability, and tortuosity of porous media from images by deep learning," *Scientific Reports. Nature Research*, 10 (*1*) 1–11 (2020). doi.org/10.1038/s41598-020-78415-x
20) L.M. Anovitz, and D.R. Cole, "Characterization and analysis of porosity and pore structures," *Reviews in Mineralogy and Geochemistry*, 80 (*1*) 61–164 (2015). doi.org/10.2138/rmg.2015.80.04
21) A. Koponen, M. Kataja, and J. Timonen, "Permeability and effective porosity of porous media," *Statistical Physics, Plasmas, Fluids, and Related Interdisciplinary Topics*, 56 (3) 3319–3325 (1997). doi.org/ 10.1103/PhysRevE.56.3319
22) J. Park, J.H. Shin, and J.K. Park, "Experimental Analysis of Porosity and Permeability in Pressed Paper." *Micromachines*, 7 (*3*) 48 (2016). doi.org/10.3390/mi7030048
23) B.M. Cummins, R. Chinthapatla, F.S. Ligler, and G.M. Walker, "Time Dependent Model for Fluid Flow in Porous Materials with Multiple Pore Sizes," *Anal. Chem*. UTC, 89 58 (2017). doi.org/10.1021/acs.analchem.6b04717
24) T. Kokalj, Y. Park, M. Vencelj, M. Jenko, and L.P. Lee, "Self-powered Imbibing Microfluidic Pump by Liquid Encapsulation: SIMPLE," *Lab Chip,* 14 (*22*) 4329-4333 (2014). doi.org/ doi.org/10.1039/C4LC00920G
25) F. Dal Dosso, T. Kokalj, J. Belotserkovsky, D. Spasic, and J. Lammertyn, "Self-powered infusion microfluidic pump for ex vivo drug delivery," *Biomed Microdevices,* 20 (*2*) 44 (2018). doi.org/10.1007/s10544-018-0289-1
26) Y. Xia, and G.M. Whitesides, "Soft Lithography," *Annual Review of Materials Science,* 28 (*1*) 153-184 (1998). doi.org/10.1146/annurev.matsci.28.1.153
27) P.K. Yuen, and V.N. Goral, "Low-cost rapid prototyping of flexible microfluidic devices using a desktop digital craft cutter," *Lab Chip,* 10 (*3*) 384-387 (2010). doi.org/10.1039/B918089C
28) M. Islam, R. Natu, and R. Martinez-Duarte, "A study on the limits and advantages of using a desktop cutter plotter to fabricate microfluidic networks," *Microfluidics and Nanofluidics,* 19 (*4*) 973-98 (2015). doi.org/10.1007/s10404-015-1626-9
29) J.I. Martínez-López, M. Mojica, C. Rodriguez, and H. Siller, "Xurography as a Rapid Fabrication Alternative for Point-of-Care Devices: Assessment of Passive Micromixers," *Sensors,* 16 705 (2016). doi.org/10.3390/s16050705
30) Z. Ihsani, "Porosity Analysis Procedure with ImageJ." n.d. (Accessed April 23, 2021).
31) AATCC, 2011. Test Method of Horizontal Wicking of Textiles. Research Triangle Park, N.C., USA.
32) B.D. MacDonald, "Flow of liquids through paper," *Journal of Fluid Mechanics*. Cambridge University Press, 852 1–4 (2018). doi.org/10.1017/jfm.2018.536
33) C.T. Rueden, J. Schindelin, M.C Hiner, B.E. DeZonia, A.E. Walter, E.T. Arena, and K.W. Eliceiri, "ImageJ2: ImageJ for the next generation of scientific image data," *BMC Bioinformatics,* 18 (*1*) 529 (2017). doi.org/10.1186/s12859-017-1934-z
34) Z. Cui, Y. Huang, and H. Liu, "Predicting the mechanical properties of brittle porous materials with various porosity and pore sizes," *Journal of the Mechanical Behavior of Biomedical Materials*, 71 10–22 (2017). doi.org/ 10.1016/j.jmbbm.2017.02.014
35) S. Priyalatha, and D. Raja, "An Overview on Objective Evaluation of Wicking Property of the Textile Material Used in Sports" *Trends in Textile Engineering & Fashion Technology,* 2 (*4*) (2018) doi.org/ 10.31031/TTEFT.2018.02.000541
36) C.B. Simile, "Critical Evaluation of Wicking in Performance Fabrics," Master of Science Thesis, Georgia Institute of Technology, 2004. http://hdl.handle.net/1853/4912
37) R. Masoodi, K.M. Pillai, and P.P. Varanasi, "Effect of externally applied liquid pressure on wicking in paper wipes," *Journal of Engineered Fibers and Fabrics,* 5 (*3*) 49–66 (2010). doi.org/ 10.1177/155892501000500307